

Geophysical Research Letters

RESEARCH LETTER

10.1029/2021GL092509

Key Points:

- Both severe ozone loss and surface warming over the Siberian Arctic were observed in the spring of 2020
- The ozone loss in the Siberian Arctic may contribute to the most of the surface warming in April by modifying the cloud radiative effects
- Ice-albedo feedback further amplifies the surface warming in April and May

Supporting Information:

Supporting Information may be found in the online version of this article.

Correspondence to:

C. Zhao,
czhao@bnu.edu.cn

Citation:

Xia, Y., Hu, Y., Huang, Y., Zhao, C., Xie, F., & Yang, Y. (2021). Significant contribution of severe ozone loss to the Siberian-Arctic surface warming in spring 2020. *Geophysical Research Letters*, 48, e2021GL092509. <https://doi.org/10.1029/2021GL092509>

Received 11 JAN 2021

Accepted 11 APR 2021

Significant Contribution of Severe Ozone Loss to the Siberian-Arctic Surface Warming in Spring 2020

Yan Xia^{1,2} , Yongyun Hu³ , Yi Huang⁴ , Chuanfeng Zhao¹ , Fei Xie¹ , and Yikun Yang¹ 

¹College of Global Change and Earth System Science, Beijing Normal University, Beijing, China, ²Key Laboratory of Middle Atmosphere and Global Environment Observation, Institute of Atmospheric Physics, Chinese Academy of Sciences, Beijing, China, ³Laboratory for Climate and Ocean-Atmosphere Studies, Department of Atmospheric and Oceanic Sciences, School of Physics, Peking University, Beijing, China, ⁴Department of Atmospheric and Oceanic Sciences, McGill University, Montreal, QC, Canada

Abstract Severe ozone loss and significant surface warming anomalies in the Siberian Arctic were observed in spring 2020. Here, we show that the anomalous surface warming was likely related to the ozone loss. The dramatic Arctic ozone loss in March was shifted to Siberia in April and May, which largely cools the lower stratosphere and leads to an increase of high clouds by modifying the static stability in the upper troposphere. This further results in an increase of longwave radiation at surface which likely contributes to surface warming. Multiple linear regression demonstrates that ozone loss contributes most of the surface warming in April, while the Arctic Oscillation and ice-albedo feedback play a minor role. In May, both ozone loss and ice-albedo feedback contribute to the surface warming. These results support that surface warming in the Siberian Arctic could occur in April and May when severe ozone loss occurs in March.

Plain Language Summary Anomalous surface warming in the Siberian Arctic was observed in spring 2020. The key question is what caused the surface warming. Here, we show that this surface warming in the Siberian Arctic is likely caused by the local severe ozone loss, along with the ice-albedo feedback. The reduction of stratospheric ozone leads to lower stratospheric cooling and a decrease in the static stability in the upper troposphere, which results in an increase in high clouds. It consequently causes an increase of surface longwave radiation and enhanced surface warming in April and May. The ice-albedo feedback further amplifies surface warming.

1. Introduction

There was an unusual warmth with global attention in the Siberian Arctic from January through June 2020. It had a prominent effect that led to record-low sea ice in the adjacent Kara and Laptev Seas, an abnormal wildfire season, thawing permafrost, and even changes in ecosystem. Overland and Wang (2020) indicates that the extreme positive Arctic Oscillation (AO) induced by the record-strong stratospheric polar vortex was the proximate cause for the warm extremes from January through April 2020.

The first Arctic “ozone hole” was observed in March and April 2020 (Dameris et al., 2020; Hu, 2020; Lawrence et al., 2020; Manney et al., 2020; Rao & Garfinkel, 2020). This severe ozone loss was closely related to an extremely strong and cold polar vortex due to weak tropospheric wave activities (Lawrence et al., 2020; Manney et al., 2020; Rao & Garfinkel, 2020). It is important to note that stratospheric ozone changes can also impact surface temperature through radiative effects (Maleska et al., 2020; Xia et al., 2016, 2018; Xia, Hu, et al., 2020; Xie et al., 2016, 2017). Xia et al. (2018) found that the changes in upper tropospheric and lower stratospheric ozone significantly influence the static stability in the upper troposphere and consequent variations of high clouds, which further impact the longwave radiation at surface. Stratospheric ozone-induced cloud radiative effects result in significant change in Antarctic sea ice, which are comparable to that due to atmospheric and oceanic dynamic processes (Xia, Hu, et al., 2020).

Recent research has determined that low ozone extremes in the Arctic may contribute to enhanced Arctic surface warming in spring through a positive longwave cloud radiative effect during the late twentieth century (Maleska et al., 2020). An important question is whether the severe ozone depletion in the spring 2020 may contribute to the anomalous surface warming in the Siberian Arctic. Here, we find the severe ozone

loss in the Siberian Arctic may play an important role in surface warming in April and May 2020, which is consistent with previous studies which have identified significant climate impacts of extreme Arctic ozone depletion in April–May by model simulations and statistical analysis (Calvo et al., 2015; Ivy et al., 2017; Smith & Polvani, 2014).

In this study, we first show observational results of the extreme Arctic ozone loss and surface warming in the spring 2020. Next, we analyze how the surface warming is related to severe ozone loss. Then, we attribute the surface warming to the Arctic Oscillation, ozone loss, and albedo feedback using the method of multiple linear regression.

2. Data and Methods

The monthly mean total column ozone is from the Multi Sensor Re-analysis version 2 (MSR-2) over 1979–2020 (Van Der A et al., 2015a, 2015b). The MSR-2 with horizontal resolution of $0.5^\circ \times 0.5^\circ$ is constructed using all available satellite observations, surface Brewer and Dobson observations, with a data assimilation model. The unit of total column ozone is the Dobson Unit (DU).

We use the National Aeronautics and Space Administration (NASA) Goddard Institute for Space Studies (GISS) Surface Temperature Analysis version 4 (GISTEMP v4) from 1979 through June 2020 to investigate the surface warming in the Siberian Arctic. The monthly mean GISTEMP v4, consisting of NOAA Global Historical Climatology Network version 4 (GHCN v4) from thousands of weather stations around the world and Extended Reconstructed Sea Surface Temperature version 5 (ERSST v5) for ocean areas, is on a $2^\circ \times 2^\circ$ grid with spatial completeness enhanced using statistical methods (Hansen et al., 2010; Lenssen et al., 2019).

Monthly mean temperature, water vapor, and cloud fraction from ERA5 reanalysis over 1979–2020 are used here. ERA5 reanalysis combines model data with observations from across the world into a globally complete and consistent data set, at a horizontal resolution of $0.25^\circ \times 0.25^\circ$ (Hersbach et al., 2020).

The monthly AO index over 1979–2020 produced by NOAA Climate Prediction Center is used for the attribution analysis. The data is available at https://www.cpc.ncep.noaa.gov/products/precip/CWlink/daily_ao_index/ao.shtml. We generate anomalies for each month by removing the climatology averaged over 1981–2010.

To quantify the impact of radiative feedback on the surface temperature anomaly in 2020, we calculate the radiative feedback at surface using the radiative kernel method introduced by Huang et al. (2017). The radiative kernel, K_X , is precalculated by a partial perturbation method using a rapid radiative transfer model, RRTM (Mlawer et al., 1997) for temperature (T), water vapor (q), and albedo (a). For the noncloudy climate variables, the radiative feedback is computed as

$$\Delta_X R = K_X \Delta X$$

for $X = T, q, \text{ or } a$. Because of the cloud masking of temperature, water vapor, and albedo feedback, the cloud feedback is then calculated following Equation 25 in Soden et al. (2008):

$$\Delta_{cl} R = \Delta CRF + (K_T^0 - K_T) \Delta T + (K_q^0 - K_q) \Delta q + (K_a^0 - K_a) \Delta a + (G^0 - G)$$

where ΔCRF is the cloud radiative forcing defined as the difference in the surface radiative fluxes between all-sky and clear-sky conditions, the K^0 and K are the clear-sky and all-sky kernels, and G^0 and G are the clear-sky and all-sky forcing. To better quantify the cloud radiative feedback, ΔCRF is computed by Clouds and the Earth's Radiant Energy System (CERES) Energy Balanced and Filled (EBAF) surface monthly mean radiation fluxes edition 4.1 (Wielicki et al., 1996). All the radiative fluxes are defined to be downward positive.

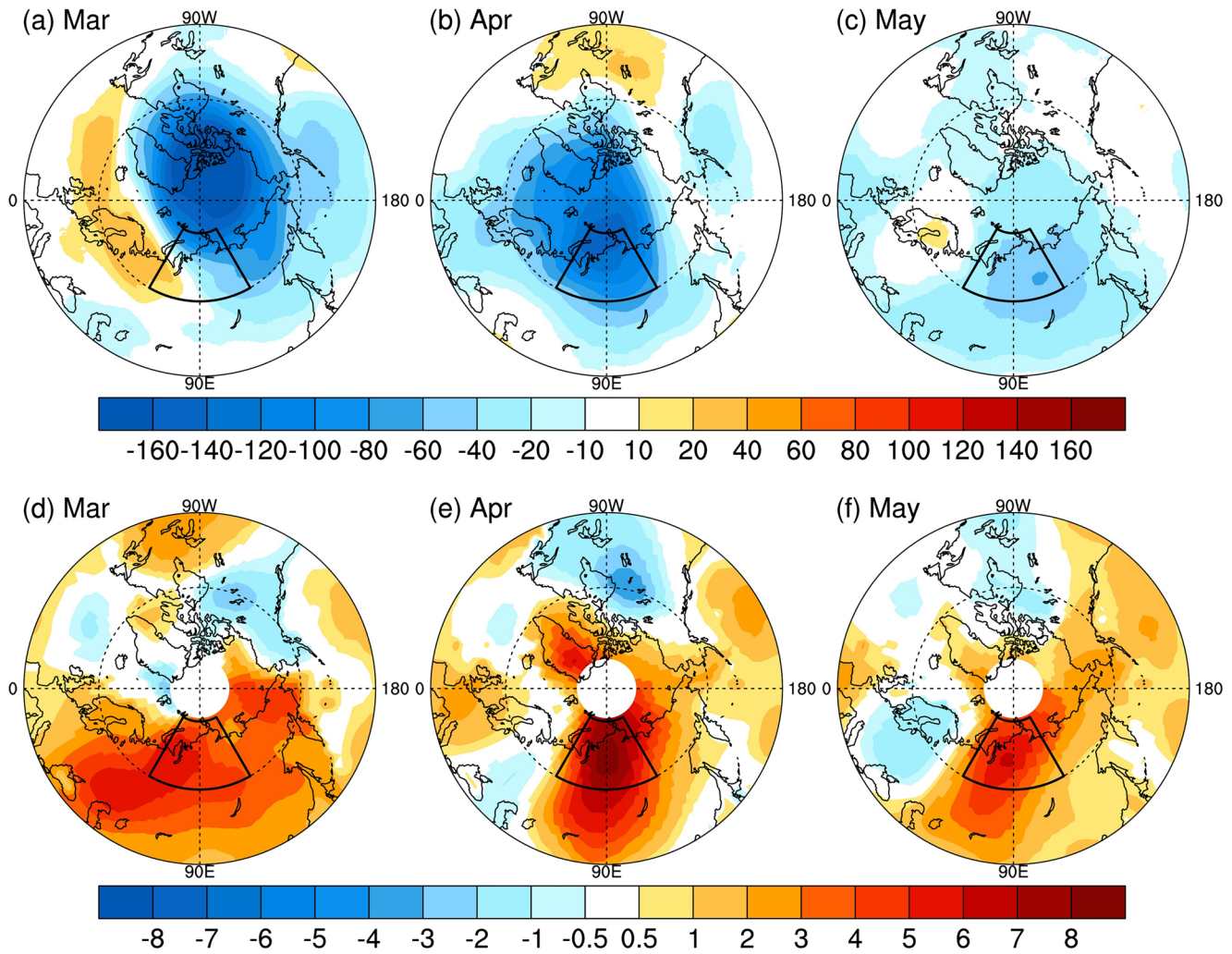


Figure 1. Geographic distributions of ((a)–(c)) total column ozone and ((d)–(f)) surface temperature anomalies in March, April, and May 2020. In plots ((a)–(c)), the units are DU. In plots ((d)–(f)), the units are K. Black boxes indicate the concerned Siberian Arctic region over 60°–80°N and 60°–120°E. DU, Dobson Unit.

3. Results

3.1. Arctic Ozone Loss and Surface Warming in the Spring 2020

Figure 1 shows spatial distributions of total column ozone and surface temperature anomalies over the Northern Hemisphere middle and high latitudes in March, April, and May 2020. It is found that ozone loss persisted from March to May in the Arctic (Figures 1a–1c). The maximum of the severe ozone depletion in March, which reaches about 201 DU, is located over the Beaufort Sea near northern North America. It is interesting to note that the maximum is shifted toward Siberia in April and located over the Kara Sea, with a value of about 157 DU. The ozone loss in May is located over central Siberia, with a maximum value of about 62 DU. The surface warming in March, which stretched across much of northern Eurasia, is mainly located over the western Russia with a maximum value of about 2.9 K (Figure 1d). Both the surface warming in April and May is located in center Siberia (Figures 1e and 1f). The maximums of the warming located in the Siberian Arctic over 60°–80°N and 60°–120°E are 8.8 K and 6.2 K in April and May, respectively. Interestingly, the ozone loss and surface warming show high spatial consistency in April and May. The spatial correlation coefficients between ozone loss and surface warming over 45°–80°N and 60°–120°E are -0.82 and -0.60 in April and May, respectively. Similar results can also be seen in spring 2011 when

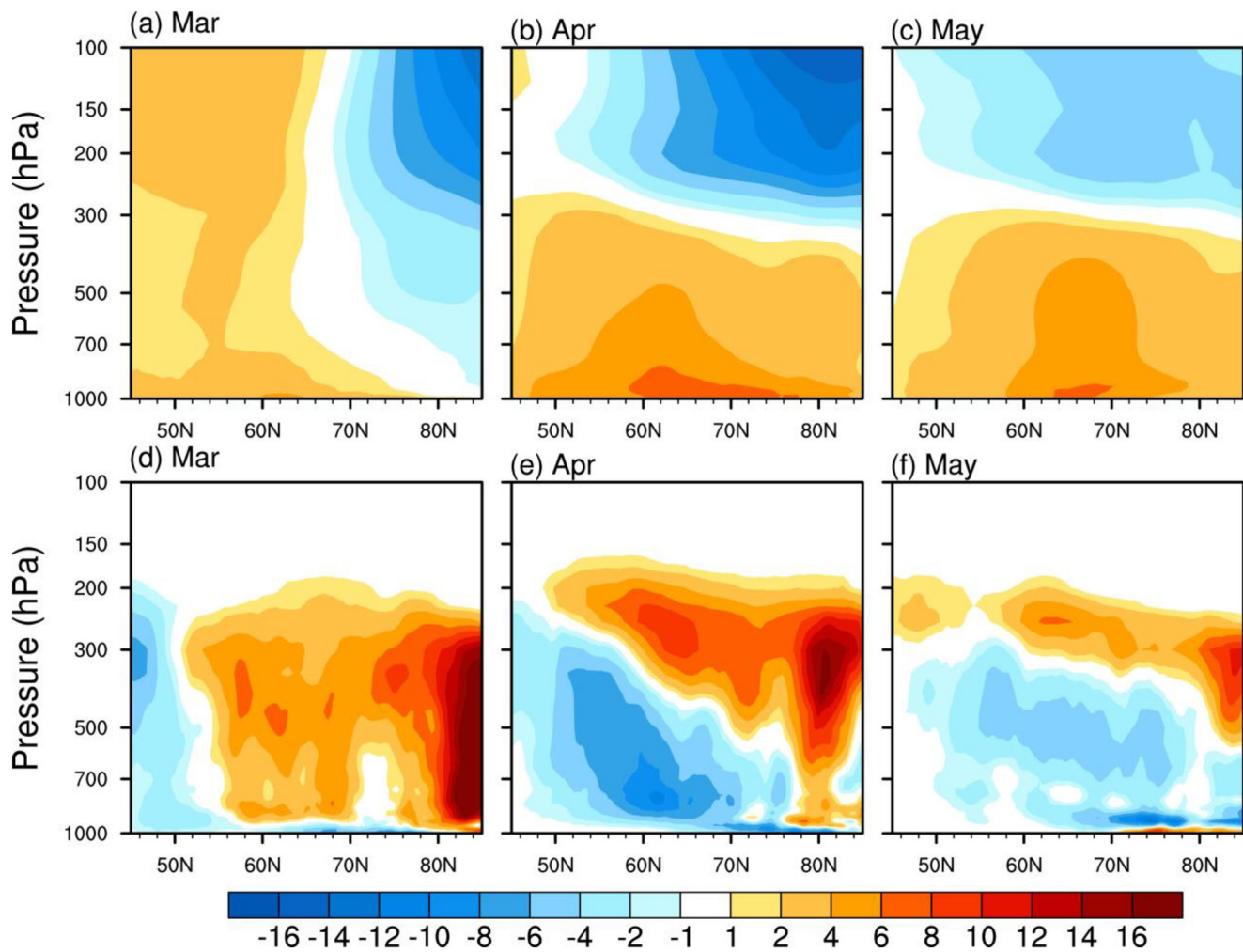


Figure 2. Vertical cross-section of ((a)–(c)) temperature and ((d)–(f)) cloud anomalies averaged over 60°–120°E in March, April, and May 2020. In plots ((a)–(c)), the units are K. In plots ((d)–(f)), the units are %.

the last severe ozone loss occurred, expect for that the ozone loss in May 2011 is much weaker than that in May 2020 (Figure S1).

Figure 2 shows the vertical cross-section of temperature and cloud anomalies averaged over 60°–120°E in March, April, and May 2020. We find that stratospheric cooling in March, which is located north of 70°N, expands southward to about 50°N of central Siberia in April and May (Figures 2a–2c). Meanwhile, the maximum of surface warming is shifted poleward from 50°–60°N to about 60°–70°N. The warm anomalies in the troposphere decrease with increasing altitude, while the magnitude of stratospheric cooling increases with increasing altitude from the tropopause region at about 300 hPa. It results in an increase in vertical temperature gradient which is the largest at the tropopause region and consequent decreases of static stability in the upper troposphere. The changes in static stability further lead to an increase of high clouds at around 300 hPa especially in April and May (Figures 2d–2f), which is consistent with the results in the previous studies (Li & Thompson, 2013; Nowack et al., 2015; Xia et al., 2016, 2018; Xia, Hu, et al., 2020). The correlation analysis further demonstrates that ozone significantly impacts the Arctic high clouds (Figure S2). It is interesting to note that the increase of high clouds reaches its maximal value over the region about 60°–70°N where the maximum of surface warming occurs. It seems that the greenhouse effects of high clouds by trapping longwave radiation may contribute to part of the surface warming in the Siberian Arctic especially in April and May, which can also be seen in April 2011 (Figure S3).

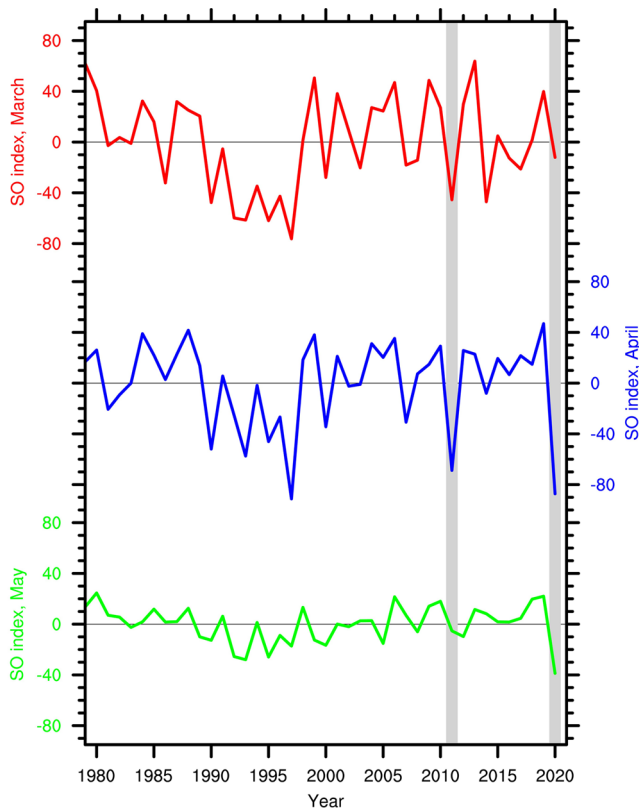


Figure 3. Time series of the SO index in March (red), April (blue), and May (green) over 1979–2020. The units are DU. Two gray-filled bars indicate 2 years of severe ozone loss in 2011 and 2020. DU, Dobson Unit; SO, Siberian ozone.

Figure 3 shows the time series of the SO index in March, April, and May over 1979–2020. The SO index has a much larger interannual variability in both March and April than that in May. It shows little trend in March and April over 1998–2020, in contrast to the significant negative trend over 1979–1997 due to the increase of ozone depleting substances (ODSs) in the late twentieth century (WMO, 2018). It is interesting to note that severe Arctic ozone depletion occurred in spring 2020 and 2011, although ODSs have been declining since the late 1990s. The SO index, which represents the ozone change over the Siberian Arctic, is about -12 , -87 , and -39 DU in March, April, and May 2020, respectively, and it is -45 , -69 , and -5 DU in March, April, and May 2011, respectively. The radiative effect of ozone depletion caused anomalously low polar temperatures and thus enhanced Arctic polar vortex (Hu & Xia, 2013; Lawrence et al., 2020). The persistent strength of the stratospheric polar vortex was accompanied by an exceptionally positive phase of the AO in the troposphere during March and April in both 2020 and 2011 (Figure S7). The AO index is about 1.6, 0.8, and 0.1 in March, April, and May 2020, respectively, and 1.0, 2.0, and -0.1 in March, April, and May 2011, respectively. In contrast to SO and AO indexes, the albedo index has much smaller interannual

To quantify the greenhouse effect of high clouds, we calculate the longwave cloud feedback at surface and find large positive cloud radiative forcing over the Siberian Arctic in April and May 2020 (Figures S4a–S4c). The maximum values of the cloud-induced longwave radiation anomalies are larger than 50 W m^{-2} , and the longwave radiative effects averaged over 60° – 80°N and 60° – 120°E are 37 and 29 W m^{-2} in April and May, respectively. This is consistent with the increase of high clouds in April and May. The increases in high clouds in March and April 2011 (Figures S3d and S3e) also result in positive cloud longwave radiative effects in March and April (Figures S4d and S4e).

3.2. Attribution of the Surface Warming

In this section, we perform attribution analysis to reveal what caused the surface warming over the Siberian Arctic in spring 2020. Following Xia, Xu, et al. (2020), we use the method of multiple linear regression to attribute the respective contributions of the AO, total ozone over central Siberia, and surface albedo to surface temperature changes. The AO index is widely used to express the impact of the large-scale atmospheric circulation on surface temperature in the NH high latitudes (Thompson & Wallace, 2000; Thompson et al., 2002). It is widely accepted that the positive AO is associated with positive surface temperature anomalies throughout high latitudes of Eurasia especially during January–March. We use the AO index over 1979–2020 to represent its effect on surface temperature. Here, the attribution analysis for year 2020 is performed using a model trained on the years 1979–2019.

The above analysis has shown that the ozone loss over central Siberia is associated with lower-stratospheric cooling and increases in high clouds, which further impacts surface longwave radiation and surface temperature. The radiation analysis further demonstrates that the positive longwave cloud feedback and albedo feedback are the two major factors affecting surface temperature over Siberian Arctic in April and May 2020 (Figures S5 and S6). Here, we define the Siberian ozone (SO) index over 1979–2020 as the area-weighted spatial-mean total ozone over 60° – 80°N and 60° – 120°E to represent the ozone effect on surface warming. The thawing of ice-rich permafrost and snow over the Siberian Arctic in the late spring due to the surface warming may result in a decrease in surface albedo, which can also influence surface temperature. To denote the albedo effects, an “albedo index” is defined as the area-weighted spatial-mean surface albedo over 60° – 80°N and 60° – 120°E from the ERA5 reanalysis. Linear trends and averages over 1979–2019 for all the three indexes are removed because we mainly focus on the interannual variability. The attribution for each factor is calculated as the index in 2020 multiplied by the corresponding regression coefficient.

variability in March and April than that in May when ice-rich permafrost over Siberia melts (Figure S8). The albedo anomalies over the Siberian Arctic are about -0.09 and -0.12 in May 2020 and 2011, respectively. It is important to note that the correlation coefficients between the AO index and total column ozone are insignificant over the Siberian Arctic in April and May (Figure S9). This means that AO and SO indexes are sufficiently independent for the multiple linear regression analysis in April and May.

Figure 4 shows the correlation coefficients between the surface temperature and the three indexes over 1979–2020. The AO index is positively correlated with surface temperature throughout high latitudes of Eurasian continent in March (Figure 4a). The maximum of the positive correlation coefficients, which is about 0.81, is located over the Scandinavian Peninsula. Surface temperature over the Siberian Arctic is also highly correlated with the AO index, which can reach about 0.67. The positive correlation coefficients in April are mainly located over central Siberia, which can reach about 0.51 (Figure 4b). Interestingly, this positive center is shifted southward to around Lake Baikal outside of the Arctic region in May (Figure 4c). The correlation coefficients between the SO index and surface temperature in March have very similar spatial pattern to that for the AO index but with opposite sign (Figure 4d). It is found that the SO index is negatively correlated with surface temperature in the Siberian Arctic in March, April, and May, with minimum values of about -0.64 , -0.66 , and -0.56 , respectively (Figures 4d–4f). This means that the ozone loss over the Siberian Arctic is closely related to the surface warming, which is consistent with the above analysis. The thawing of ice-rich permafrost over the Siberian Arctic in the late spring impacts surface albedo and further feeds back to surface temperature. We find that this ice-albedo feedback mainly occurs in April and May and plays an important role in the surface temperature change (Figures 4g–4i). An increase in surface albedo reflect more solar radiation and cools the surface. Negative correlation coefficients between surface temperature and albedo index, which can reach about -0.86 , is located over the Siberian Arctic in May.

Using the method of multiple linear regression, here, we attribute surface warming over the Siberian Arctic in April and May 2020 to the positive AO, severe Siberian ozone loss, and the decrease of surface albedo (Figure 5). The attribution in March is not shown here because the significant correlations among the three indexes over 1979–2020 in March (see Figure S9 and Table S1). In April, ozone loss has the largest contribution to the observed surface warming over the Siberian Arctic, and the maximum of the contributions is about 5.1 K. The surface albedo and AO play a minor role in the warm anomalies, with maximum values of about 3.5 K and 1.4 K, respectively. The summation of the three terms explains about 98% of the observed warming. In May, it is also ozone loss that plays an important role in the observed surface warming, which contributes about 2.3 K. Ice-albedo feedback largely amplifies the surface warming by about 4.6 K. The observed warming is explained by about 95% by the three terms over the Siberian Arctic. The multiple regression analysis for 2011 shows very similar results to that for 2020 (Figure S10), expect for that the ozone change has little influence on the surface temperature in May 2011 which is consistent with the little change in ozone and high clouds in May 2011 (Figures S1c and S3f).

4. Conclusions and Discussions

The unprecedented surface warming over the Siberian Arctic in spring 2020 is investigated here. The maximum surface warming over the Siberian Arctic in April and May are up to 8.8 K and 6.2 K, respectively. We show observational evidence that this surface warming is likely related to the severe Arctic ozone depletion in spring 2020. The record Arctic ozone loss in March 2020 was shifted to central Siberia in April and May and led to local cooling in the lower stratosphere, which further results in a reduction of upper tropospheric stability and a consequent increase of high clouds. This would contribute to the enhanced surface warming over the Siberian Arctic through a positive longwave cloud radiative effect.

Multiple linear regression shows that ozone loss in the Siberian Arctic plays an important role in causing the observed warming in April and May 2020. The maximum contribution by ozone loss are up to 5.1 K and 2.3 K in April and May, respectively. It is found that the positive AO plays a minor role in the surface warming in April and the ice-albedo feedback largely amplifies the warming in April and May. Our conclusions are also supported by the analyses for 2011. The extreme ozone depletion in 1997 is also associated with surface warming in April which is not shown here. Further work is needed to examine the impact of the long-term trend of the SO index from 1979 to 1997 on the changes in surface temperature.

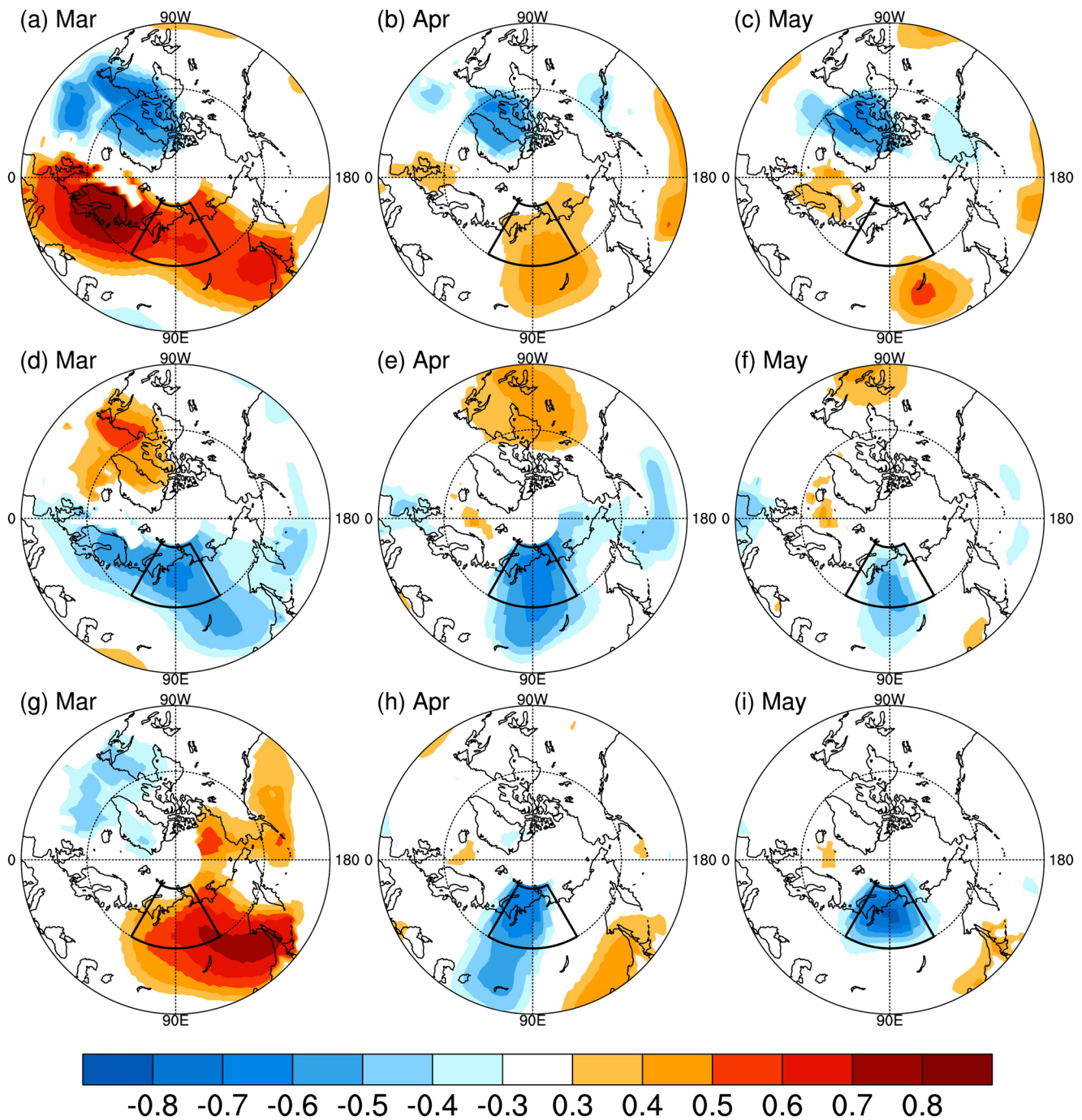


Figure 4. Geographic distributions of the correlation coefficients between surface temperature and ((a)–(c)) AO index, ((d)–(f)) SO index, and ((g)–(i)) albedo index over 1979–2020 in March, April, and May. Black boxes indicate the concerned Siberian Arctic region over 60°–80°N and 60°–120°E. The correlation coefficient of ± 0.3 corresponds to the 95% confidence level for the 42 years. SO, Siberian ozone.

In this work, we attribute the lower-stratospheric cooling and the increase of high clouds over the Siberian Arctic to ozone depletion in April and May 2020. However, we should note that stratospheric temperature and high clouds can also be impacted by the radiative effects of clouds and stratospheric water vapor, convections, and surface temperature (Ceppi et al., 2017). Therefore, attribution for the changes in high clouds needs further investigation in future.

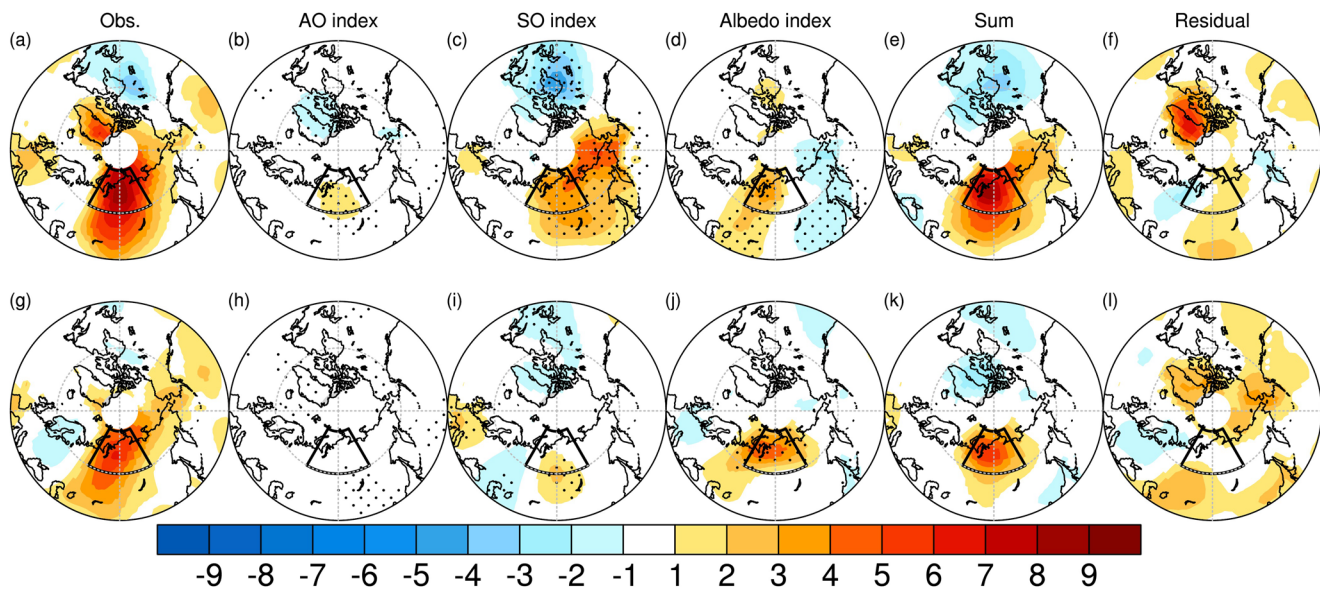


Figure 5. Multiple linear regression of observed surface temperature change in April and May 2020. Top panels: April and bottom panels: May. From left to right, the plots are observed surface temperature anomalies, surface temperature changes attributable to the AO index, surface temperature changes attributable to SO index, surface temperature changes attributable to albedo index, summation of the three terms, and the residual term, that is, the difference between the observed surface temperature changes and summation. The units are K. Regions with dots are the places where regressions have statistical significance levels higher than the 95% confidence level.

It is important to note that Arctic ozone loss in March is likely shifted to central Siberia in April and May from the correlation analysis over 1979–2020 (Figure S11), which suggests that surface warming in the Siberian Arctic would occur in April when severe ozone loss occurs in March in the future.

Data Availability Statement

The authors declare that data sets for this research are available in the following online repository. The MSR-2 observations of the total column ozone can be found at <http://www.temis.nl/protocols/O3global.html>. The NASA GISTEMP v4 can be accessed at <https://data.giss.nasa.gov/gistemp/>. The ERA5 reanalysis can be accessed at <https://cds.climate.copernicus.eu/cdsapp#!/search?type=dataset&text=ERA5>. The CERES EBAF Edition 4.1 is available at <https://opendap.larc.nasa.gov/opendap/CERES/EBAF/Edition4.1/contents.html>.

Acknowledgments

The authors thank Dr Jian Yue for helpful comments. This work is supported by the Second Tibetan Plateau Scientific Expedition and Research Program (STEP), under grant of 2019QZKK0604, Key Laboratory of Middle Atmosphere and Global environment Observation (LAGEO-2020-09), and the Fundamental Research Funds for the Central Universities. C. Zhao is supported by the National Natural Science Foundation of China (NSFC), under grant 41925022. Y. Hu is supported by the National Natural Science Foundation of China (NSFC), under grants 41530423 and 41761144072. Y. Huang acknowledges a grant from the Natural Sciences and Engineering Research Council of Canada (RGPIN-2019-04511).

References

- Calvo, N., Polvani, L. M., & Solomon, S. (2015). On the surface impact of Arctic stratospheric ozone extremes. *Environmental Research Letters*, *10*(9), 094003. <https://doi.org/10.1088/1748-9326/10/9/094003>
- Ceppi, P., Brient, F., Zelinka, M. D., & Hartmann, D. L. (2017). Cloud feedback mechanisms and their representation in global climate models. *WIREs Climate Change*, *8*(4), e465. <https://doi.org/10.1002/wcc.465>
- Dameris, M., Loyola, D. G., Nützel, M., Coldewey-Egbers, M., Lerot, C., Romahn, F., & van Roozendaal, M. (2020). First description and classification of the ozone hole over the Arctic in boreal spring 2020. *Atmospheric Chemistry and Physics Discussions*, *2020*, 1–26.
- Hansen, J., Ruedy, R., Sato, M., & Lo, K. (2010). Global Surface Temperature change. *Reviews of Geophysics*, *48*(4), RG4004. <https://doi.org/10.1029/2010rg000345>
- Hersbach, H., Bell, B., Berrisford, P., Hirahara, S., Horányi, A., Muñoz-Sabater, J., et al. (2020). The ERA5 global reanalysis. *The Quarterly Journal of the Royal Meteorological Society*, *146*(730), 1999–2049. <https://doi.org/10.1002/qj.3803>
- Hu, Y. (2020). The very unusual polar stratosphere in 2019–2020. *Science Bulletin*, *65*(21), 1775–1777. <https://doi.org/10.1016/j.scib.2020.07.011>
- Hu, Y., & Xia, Y. (2013). Extremely cold and persistent stratospheric Arctic vortex in the winter of 2010–2011. *Chinese Science Bulletin*, *58*(25), 3155–3160. <https://doi.org/10.1007/s11434-013-5945-5>
- Huang, Y., Xia, Y., & Tan, X. (2017). On the pattern of CO2 radiative forcing and poleward energy transport. *Journal of Geophysical Research: Atmosphere*, *122*(20), 10578–10593. <https://doi.org/10.1002/2017jd027221>
- Ivy, D. J., Solomon, S., Calvo, N., & Thompson, D. W. J. (2017). Observed connections of Arctic stratospheric ozone extremes to Northern Hemisphere surface climate. *Environmental Research Letters*, *12*(2), 024004. <https://doi.org/10.1088/1748-9326/aa57a4>

- Lawrence, Z. D., Perlwitz, J., Butler, A. H., Manney, G. L., Newman, P. A., Lee, S. H., & Nash, E. R. (2020). The remarkably strong arctic stratospheric polar vortex of winter 2020: Links to record-breaking arctic oscillation and ozone loss. *Journal of Geophysical Research: Atmosphere*, *125*(22), e2020JD033271. <https://doi.org/10.1029/2020jd033271>
- Lenssen, N. J. L., Schmidt, G. A., Hansen, J. E., Menne, M. J., Persin, A., Ruedy, R., & Zyss, D. (2019). Improvements in the GISTEMP uncertainty model. *Journal of Geophysical Research: Atmospheres*, *124*(12), 6307–6326. <https://doi.org/10.1029/2018jd029522>
- Li, Y., & Thompson, D. W. J. (2013). The signature of the stratospheric Brewer-Dobson circulation in tropospheric clouds. *Journal of Geophysical Research: Atmospheres*, *118*(9), 3486–3494. <https://doi.org/10.1002/jgrd.50339>
- Maleska, S., Smith, K., & Virgin, J. (2020). Impacts of Stratospheric Ozone Extremes on Arctic High Cloud. *Journal of Climate*, *33*(20), 1–41. <https://doi.org/10.1175/jcli-d-19-0867.1>
- Manney, G. L., Livesey, N. J., Santee, M. L., Froidevaux, L., Lambert, A., Lawrence, Z. D., et al. (2020). Record-low Arctic stratospheric ozone in 2020: MLS observations of chemical processes and comparisons with previous extreme winters. *Geophysical Research Letters*, *47*(16), e2020GL089063. <https://doi.org/10.1029/2020gl089063>
- Mlawer, E. J., Taubman, S. J., Brown, P. D., Iacono, M. J., & Clough, S. A. (1997). Radiative transfer for inhomogeneous atmospheres: RRTM, a validated correlated-k model for the longwave. *Journal of Geophysical Research*, *102*(D14), 16663–16682. <https://doi.org/10.1029/97jd00237>
- Nowack, P. J., Luke Abraham, N., Maycock, A. C., Braesicke, P., Gregory, J. M., Joshi, M. M., et al. (2015). A large ozone-circulation feedback and its implications for global warming assessments. *Nature Climate Change*, *5*(1), 41–45. <https://doi.org/10.1038/nclimate2451>
- Overland, J. E., & Wang, M. (2020). The 2020 Siberian heat wave. *International Journal of Climatology*, *41*, E2341–E2346. <https://doi.org/10.1002/joc.6850>
- Rao, J., & Garfinkel, C. I. (2020). Arctic ozone loss in march 2020 and its seasonal prediction in CFSv2: A comparative study with the 1997 and 2011 cases. *Journal of Geophysical Research: Atmosphere*, *125*(21), e2020JD033524. <https://doi.org/10.1029/2020jd033524>
- Smith, K. L., & Polvani, L. M. (2014). The surface impacts of Arctic stratospheric ozone anomalies. *Environmental Research Letters*, *9*(7), 074015. <https://doi.org/10.1088/1748-9326/9/7/074015>
- Soden, B. J., Held, I. M., Colman, R., Shell, K. M., Kiehl, J. T., & Shields, C. A. (2008). Quantifying climate feedbacks using radiative kernels. *Bulletin of the American Meteorological Society*, *21*(14), 3504–3520. <https://doi.org/10.1175/2007jcli2110.1>
- Thompson, D. W. J., Baldwin, M. P., & Wallace, J. M. (2002). Stratospheric connection to Northern Hemisphere wintertime weather: Implications for prediction. *Journal of Climate*, *15*(12), 1421–1428. [https://doi.org/10.1175/1520-0442\(2002\)015<1421:sctnhw>2.0.co;2](https://doi.org/10.1175/1520-0442(2002)015<1421:sctnhw>2.0.co;2)
- Thompson, D. W. J., & Wallace, J. M. (2000). Annular modes in the extratropical circulation. Part I: Month-to-month variability*. *Journal of Climate*, *13*(5), 1000–1016. [https://doi.org/10.1175/1520-0442\(2000\)013<1000:amitec>2.0.co;2](https://doi.org/10.1175/1520-0442(2000)013<1000:amitec>2.0.co;2)
- Van Der A, R., Allaart, M. A. F., & Eskes, H. (2015). Extended and refined multi sensor reanalysis of total ozone for the period 1970–2012. *Atmospheric Measurement Techniques*, *8*(7), 3021–3035. <https://doi.org/10.5194/amt-8-3021-2015>
- Van Der A, R., Allaart, M. A. F., & Eskes, H. (2015). *Multi-Sensor Reanalysis (MSR) of total ozone, version 2*. Royal Netherlands Meteorological Institute (KNMI).
- Wielicki, B. A., Barkstrom, B. R., Harrison, E. F., Lee, R. B., III, Louis Smith, G., & Cooper, J. E. (1996). Clouds and the Earth's Radiant Energy System (CERES): An earth observing system experiment. *Bulletin of the American Meteorological Society*, *77*(5), 853–868. [https://doi.org/10.1175/1520-0477\(1996\)077<0853:catere>2.0.co;2](https://doi.org/10.1175/1520-0477(1996)077<0853:catere>2.0.co;2)
- WMO. (2018). *Scientific assessment of ozone depletion: 2018, global ozone research and monitoring project–report No. 58*, p. 588. Geneva, Switzerland.
- Xia, Y., Hu, Y., & Huang, Y. (2016). Strong modification of stratospheric ozone forcing by cloud and sea-ice adjustments. *Atmospheric Chemistry and Physics*, *16*(12), 7559–7567. <https://doi.org/10.5194/acp-16-7559-2016>
- Xia, Y., Hu, Y., Liu, J., Huang, Y., Xie, Y., & Lin, J. (2020). Stratospheric ozone-induced cloud radiative effects on Antarctic sea ice. *Advances in Atmospheric Sciences*, *37*(5), 505–514. <https://doi.org/10.1007/s00376-019-8251-6>
- Xia, Y., Huang, Y., & Hu, Y. (2018). On the climate impacts of upper tropospheric and lower stratospheric ozone. *Journal of Geophysical Research: Atmospheres*, *123*, 730–739. <https://doi.org/10.1002/2017jd027398>
- Xia, Y., Xu, W., Hu, Y., & Xie, F. (2020). Southern-Hemisphere high-latitude stratospheric warming revisit. *Climate Dynamics*, *54*, 1671–1682. <https://doi.org/10.1007/s00382-019-05083-7>
- Xie, F., Li, J., Tian, W., Fu, Q., Jin, F.-F., Hu, Y., et al. (2016). A connection from Arctic stratospheric ozone to El Niño-Southern oscillation. *Environmental Research Letters*, *11*(12), 124026. <https://doi.org/10.1088/1748-9326/11/12/124026>
- Xie, F., Li, J., Zhang, J., Tian, W., Hu, Y., Zhao, S., et al. (2017). Variations in North Pacific sea surface temperature caused by Arctic stratospheric ozone anomalies. *Environmental Research Letters*, *12*(11), 114023. <https://doi.org/10.1088/1748-9326/aa9005>